The Curvature of dA Tracts Is Temperature Dependent†

Bozidar Jerkovic and Philip H. Bolton*

Chemistry Department, Wesleyan University, Middletown, Connecticut 06459

Received June 26, 2000; Revised Manuscript Received August 22, 2000

ABSTRACT: The curvature of dA tracts has been proposed to be important in the recognition, packaging, and regulation of DNA. The effects of dA tracts on the gel mobility, rate of cyclization, and other properties of DNA have been extensively studied. The consensus value for the curvature induced by a single dA tract is about 18°. There are two main competing models for the origin of the curvature of dA tracts. One model assigns the central role to sequence-dependent steric clashes and the other to sequence dependent interactions with cations. The temperature dependence of the shape functions, the molecule specific part of the diffusion coefficients, of a set of six DNAs has been examined here. The set contains DNAs with dA tracts in or out of phase with respect to the helical repeat as well as those with scrambled dA-dT regions. The results show that the curvature of dA tracts is highly temperature dependent and that the curvature is largely melted out by 40 °C. The curvature melts out before there is significant premelting, or breathing of the dA tracts or the scrambled dA-dT regions. The curvature does not appear to reach a plateau value at low temperatures. A qualitative model for the melting of the curvature of dA tracts is proposed.

The means used to recognize a wide range of DNA damage by repair and cell cycle checkpoint systems are poorly understood. We have proposed that flexibility can be used as a global means of recognition of damaged DNA and have shown that damaged and mismatched sites can increase the flexibility of DNA (*1*, *2*). The comparison of the diffusion properties of DNAs allows monitoring their relative flexibility (*1*, *2*). The flexibility, or ease of bending, of DNA is also important in its packaging and its recognition by transcription factors and other proteins, as well as in its interactions with ligands, including drug molecules (*1*−*17*). Since both flexibility and curvature effect the diffusion of DNA, methods are needed to separate out the contributions from each factor.

The curvature of DNA is thought to be important in DNA packaging and in DNA−protein interactions (*2*, *3*, *6*, *7*, *10*, *15*−*38*). This investigation aims to gain additional information about the curvature and flexibility of DNAs containing dA tracts and how these properties vary with changes in temperature to evaluate the possible relevance of dA tract curvature in biological systems. The effects of temperature on the curvature and flexibility of dA tracts have not been well characterized. The effects of the curvature need to be characterized before dA tracts can be used to determine the curvature of damaged and mismatched sites.

The mechanism of the curvature of dA tract DNAs remains controversial (*39*, *40*). One model proposes that steric clashes and other interactions between adjacent residues are the main forces that give rise to the sequence-dependent bending of DNA (*39*). The competing model proposes that the variation in neutralization of the backbone phosphates due to sequence dependent interactions with cations is the prime determinant of DNA curvature (*40*). Both approaches treat the curvature primarily as a sequence-dependent property and not as a function of temperature.

Diffusion coefficients, *D*, of DNA can be measured to high precision and reproducibility by NMR methods under a wide range of experimental conditions (*1*, *2*, *41*). This methodology also has the potential to be applied to complexes of DNA with small molecule ligands, including cations, and proteins. For example, the effect of netropsin and similar molecules (*42*−*46*) on the curvature of dA tract DNAs could be examined by this approach. Diffusion coefficients depend on a Boltzmann factor and on the viscosity of the solution, which is temperature dependent. Thus, diffusion coefficients are not the most suitable monitors of DNA flexibility and curvature. The shape function, $S_f = \eta D/T$ with η the solvent viscosity, does not have the viscosity and temperature dependence of the diffusion coefficients (*2*). The temperature dependence of a shape function reports on the changes in the curvature and flexibility of the DNA rather than on changes in the solvent viscosity or other nonspecific temperature effects. The DNAs with more compact structures will have larger shape functions than those with more extended structures. For example, a curved duplex DNA will have a larger shape function than a straight DNA of the same length.

We have shown that DNAs with a damaged or mismatched site have larger shape functions than fully complementary DNA at low temperatures due to the intrinsic flexibility of the damaged or mismatched site (*1*, *2*). Mismatched sites

† This research was supported, in part, by Grant GM-51298 from the National Institutes of Health. The 500 MHz spectrometer was purchased with support from the National Science Foundation BIR-95-12478 and from the Camille and Henry Dreyfus Foundation. The 400 MHz NMR spectrometer was purchased with support from the National Science Foundation BIR 93-03077.

* To whom correspondence should be addressed. Phone: (860) 685-2668. Fax: (860) 685-2211. E-mail: pbolton@wesleyan.edu.

10.1021/bi0014507 CCC: $19.00
Published on Web 09/14/2000

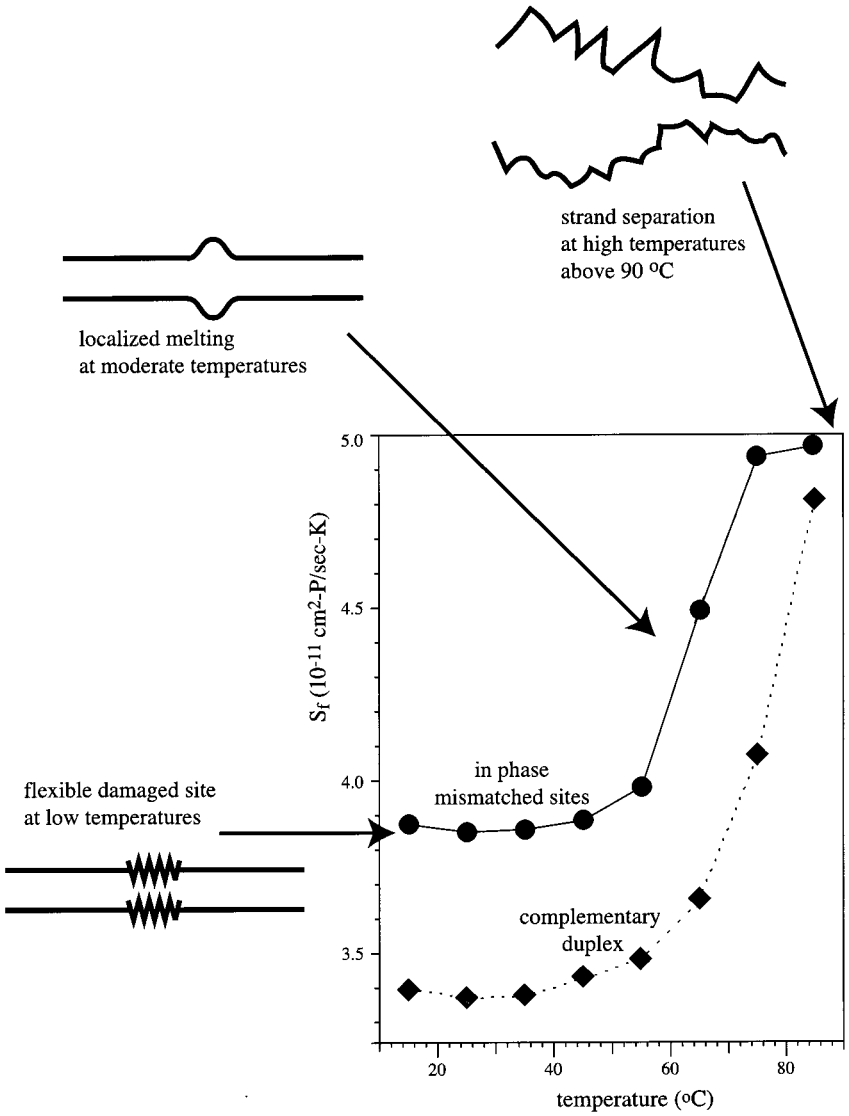

FIGURE 1: Proposed model for the effect of flexible sites, on the shape function of duplex DNA is depicted. At low temperatures the intrinsic flexibility of the mismatched site accounts for the difference in shape functions while at intermediate temperatures the localized melting of the mismatched site is dominant. At high enough temperature there is strand separation. The model is illustrated using the data on a DNA with dA-dC mismatched sites that are in phase with respect to the helical repeat and the analogous fully complementary duplex (*2*).

may have modest curvature and other damaged sites, such as thymine dimers or platinum adducts, may have significant curvature (*1*, *2*). An increase in flexibility gives rise to structures that have, as an ensemble average, a more compact structure. At high enough temperatures, there is localized melting of the duplex near the damaged or mismatched site and at even higher temperatures, the strands of the duplex DNA separate (*2*). The overall features of this qualitative model are depicted in Figure 1 for the case of mismatched sites.

To apply this methodology to curved DNA, the sequence element d(AAAAAT) has been used. The curvature of this sequence element has been examined by the structural methods of NMR (*47*) and crystallography (*48*, *49*) as well as by gel retardation, DNA cyclization, and many other approaches (*3*, *21*, *28*, *36*, *50*, *51*). The consensus bending angle is approximately 18° for each d(AAAAAT) tract.

DNAs with a single dA tract as well as DNAs with a pair, or more, of dA tracts at various phases relative to the helical repeat have been examined to separate the contributions from flexibility and curvature (*3*, *6*, *21*, *51*). When dA tracts are separated by the helical repeat and are in phase, then the effects of the curvature of the dA tracts will be largely additive (*3*, *21*). When dA tracts are separated by the helical repeat and are out of phase, then the effects of the curvature of the dA tracts will partially cancel out (*3*, *21*). The effects of the flexibility of the dA tracts will be largely additive whether the dA tracts are in or out of phase with respect to the helical repeat (*3*, *21*). The six sequences used, shown in Figure 2, contain dA tracts that are in or out of phase with respect to the helical repeat. The samples with the scrambled d(ATATAT) sequence element are expected to have minimal curvature while exhibiting similar flexibility to the DNAs with the d(AAAAAT) sequence element.

This solution state, NMR-based shape function approach has advantages relative to the other approaches previously used to monitor the curvature and flexibility of DNA. The shape function approach does not involve labeling of the DNAs or interactions of the DNAs with enzymes, gels, dyes, or other agents that may have significant interactions that

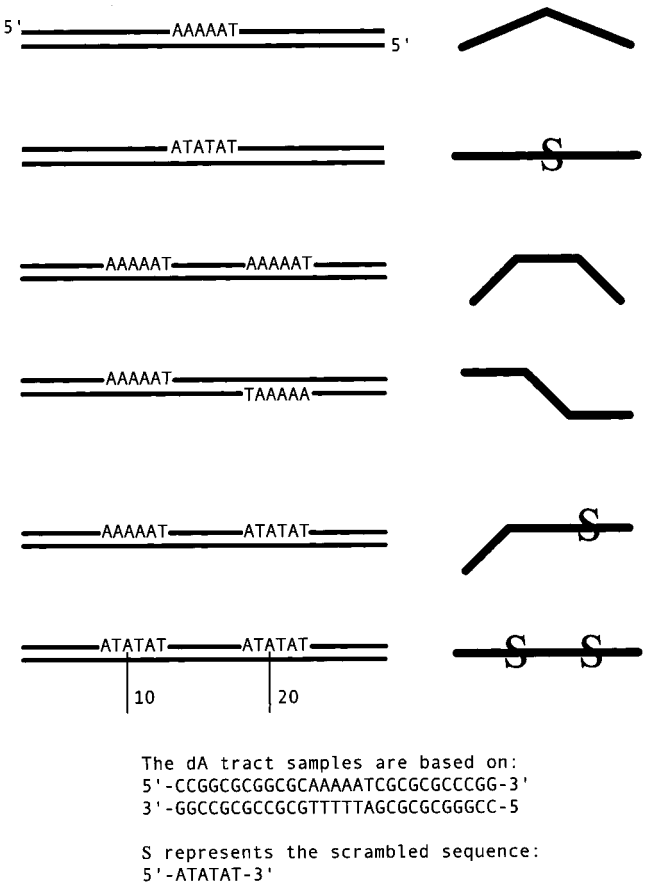

FIGURE 2: Six duplex DNAs used in this study are shown along with a depiction of the relative phasing and positioning of the dA tracts. The positions of the scrambled d(ATATAT) sequences are depicted by "S".

depend on the DNA sequence, the temperature, the buffer conditions or other factors. The NMR-based shape function methods monitor the ensemble average of the properties of the DNAs rather than being particularly sensitive to the statistically rare cases in which the ends of the DNA are spatially close to one another which is the property measured in cyclization experiments. The probability of the rare events is most sensitive to the tails of the potential energy functions that control curvature. A particular advantage of the shape function-based approach is its applicability to the same samples, under the same conditions, being used, both here and elsewhere, in NMR based structural studies of curved and damaged DNAs, including chemically fragile ones. In addition, the shape function approach could be used for the determination of the energies and mean values of the roll, tilt, and twist for free DNAs as was done using cyclization data (*50*). However, the shape function approach could also do this as a function of dye binding and as a function of changes in solvent composition including variations in cation concentration and composition.

MATERIALS AND METHODS

Sample Preparation. The 29mers were obtained from Integrated DNA Technologies Inc., Coralville, IA, and the sequences are given in Figure 2. The DNA samples were ethanol precipitated three times to remove salt, trace amounts of protecting groups, and other contaminants. NMR and HPLC-based analysis of the samples showed no detectable impurities. The single-stranded DNAs were combined to produce duplex DNAs using calculated extinction coefficients. The proton NMR spectra of the resulting samples were examined and additional titration carried out, as necessary, until there was no detectable presence of single strand material. Each of the duplex 29mer NMR samples contained a total of 27 A260 of DNA in 500 μL of 100 mM NaCl and 10 mM phosphate buffer at pH 7.0 that also contained 50 μM EDTA. One A260 is equivalent to an optical density of 1 at 260 nm in 1 cm path-length cell.

NMR Experiments and Data Processing. All of the diffusion experiments were carried out using a Varian 400 MHz UnityPlus spectrometer and a Nalorac double-resonance, pulsed field gradient, 5 mm probe. The gradient strength calibration was initially performed as described in the Nalorac probe manual. However, we have noted that the strength of the gradient varied with the gradient duration time. Therefore, the gradient strength as a function of gradient on time was determined, and the results are presented in the Supporting Information. The diffusion experiments were carried out using the PFG-STE, Pulsed Field Gradient Stimulated Echo, experiment with $\delta = 8$ ms and $\Delta = 262$ ms as described previously (*2*). The strengths of the first and third gradient pulses were the same, and the experiment was carried out with 27 different values of the variable gradient strength from 13.7 to 87.9 G/cm. The strength of the gradient used to suppress transverse magnetization, applied at the middle of the Δ period, was 13.7 G/cm.

During the initial experiments, we noticed that at lower gradient values, G between 13.7 and 22 G/cm, signal from residual ^1H_2O was present. To minimize the contribution from the water protons to the integrated intensity of the spectrum, we have incorporated a diffusion filter into the experiment as described in the Supporting Information.

For each spectrum, 5568 complex points were collected, with 600 transients, from 10 to 55 °C. A spectral width of 20 kHz and a delay time of 8 s were used. The free induction decays were Gaussian weighted, Fourier transformed, baseline corrected, and then integrated. VNMR version 6.1B software was used to acquire and process the data. A line broadening of 512 Hz was applied and integration was over all of the proton resonances of the DNAs.

The diffusion coefficients, D, were calculated from the ratio of the intensity obtained with gradient strength G, I_G, to that obtained with no gradient, I_0, by use of $I_G/I_0 = \exp[-D\gamma_H^2\delta^2G^2(\Delta - \delta/3)]$. Plots of $\ln(I_G/I_0)$ versus G^2 were fit by nonlinear least squares, the correlation coefficients determined, and the results graphed using KaleidaGraph, version 3.02, from Synergy Software as previously described (*2*). Several independent determinations were made on the same sample and the standard deviation of each was in the range of 1−2%. The standard deviation for the determination of a single data point at a particular I_G was found to be between 1 and 2%. The correlation coefficients for all of the fits of the diffusion coefficients were greater than 0.990. Representative plots of $\ln(I_G/I_0)$ versus G^2 are included in the Supporting Information.

The spectra of the imino protons were obtained using a Varian Inova 500 MHz spectrometer and are included in the Supporting Information.

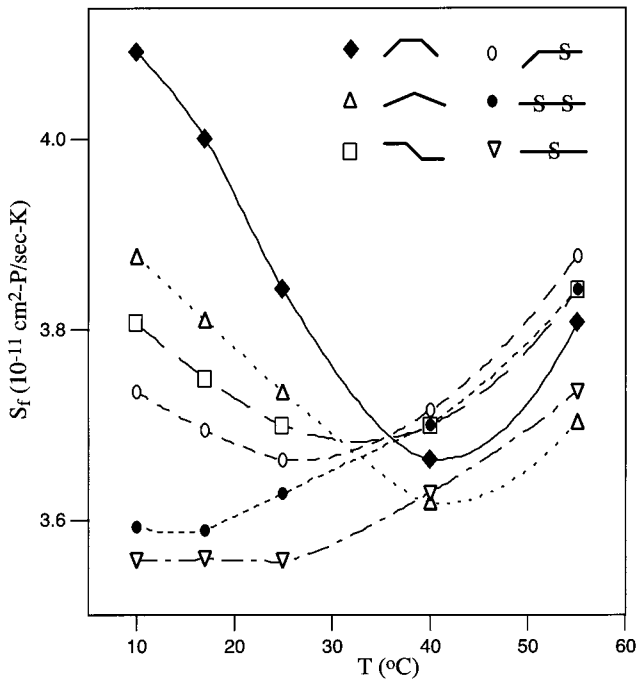

FIGURE 3: Shape functions of the six duplex DNAs are shown over the temperature range 10−55 °C. The points are connected by lines to aid visualization of the data and are not based on any model. The P denotes a "Poise" which is the unit of viscosity (g/s cm).

RESULTS AND DISCUSSION

The shape functions of each of the six DNAs were obtained at 10, 17, 25, 40, and 55 °C with the values plotted in Figure 3. The shape functions at 10 °C are in the same rank order as that observed in gel retardation experiments for analogous samples. The DNA with in phase dA tracts has the largest shape function and would have the fastest gel mobility. The DNA with a single dA tract in the middle has the next largest shape function, then the DNA with out of phase dA tracts, then the DNA with one dA tract and one scrambled sequence and then the two DNAs with scrambled sequences.

The difference between the shape function of the DNA with the in phase dA tracts and the DNAs with scrambled sequences is about 15% at 10 °C. This is comparable to the difference in shape function between an undamaged 25mer duplex and the corresponding sample with a central dA-dC mismatch (*2*). The difference in the shape functions of the DNAs with the dA tracts in and out of phase with respect to the helical repeat is approximately equal to the difference in the shape functions of the DNAs with a central dA tract and that with a central scrambled sequence. These results indicate that at 10 °C the dA tracts are curved since there is a significant difference between the shape functions of the DNAs with in and out of phase dA tracts. Similarly, the difference in the shape function between the DNA with a central dA tract and the DNA with a central scrambled sequence indicates curvature.

The qualitative model depicted in Figure 1 is based on the data that showed that mismatched sites have more intrinsic flexibility than do undamaged sites (*2*). At intermediate temperatures, there is localized melting of the DNA at the mismatched site which gives rise to increased flexibility. The temperature dependence of the shape functions was examined to determine if the curvature of the DNAs melts out at temperatures below that of the localized melting of the dA tracts. The DNAs with dA tracts and those with scrambled sequences are expected to exhibit localized melting, or breathing, as dA-dT rich regions melt at lower temperatures than do dG-dC rich regions.

The shape functions for the six DNAs are plotted in Figure 3 as a function of temperature. A striking feature is that the shape functions of the DNAs with dA tracts *decrease* with increasing temperature from 10 to about 40 °C. An increase in flexibility would give rise to an increase in the shape function. The shape function of the DNA with in phase dA tracts exhibits the largest decrease. The shape function of the DNA with a single, central dA tract is nearly the same as that of the DNA with a single, central scrambled sequence at 40 °C. These results show that the average structures of the DNAs with dA tracts become *less* compact as the temperature is raised. The decreases in shape functions for the dA tract DNAs, but not those with scrambled dA-dT regions, show that the curvature of the dA tract DNAs *decreases* as the temperature is raised.

The temperature dependence of the DNAs with one or two scrambled sequences is similar to those observed previously for duplex DNAs (*1*, *2*). The shape functions are essentially constant over the temperature range of 10−40 °C and then rise with increasing temperature. The rise is attributed to localized melting of the dA-dT regions and is more pronounced for the DNA with two, scrambled dA-dT regions than for the DNA with a single, central dA-dT region.

The DNAs with two dA-dT rich regions have larger shape functions then the DNAs with one dA-dT rich region at 55 °C. Thus, the DNA samples were divided into those with a single dA tract or single scrambled sequence and those with two. Figure 4 contains plots of the ratios of the shape functions of these two groups. The temperature dependence of the ratios of the shape functions approximates the melting of the curvature. These plots indicate that the melting of the curvature of the dA tracts is mostly complete by 40 °C. At 55 °C, the shape function differences are primarily determined by the number of dA-dT rich regions and not whether these are dA tracts or scrambled sequences.

The imino proton spectra of these DNAs have been obtained from 10 to 55 °C with the results included in the Supporting Information. The examination of the resonances of the imino protons of these DNAs indicated that there is no appreciable difference in the line widths of the imino protons of dA-dT and dG-dC base pairs at 40 °C for any of the six samples. The line widths of the dT iminos are only marginally greater than those of the dG iminos at 55 °C. This can be most clearly seen for the most upfield, all from dG residues, and most downfield resonances which are all from dT residues. These results indicate that there is little "breathing" or localized melting of the DNAs in the dA-dT rich regions at 40 °C while the curvature is melted out at this temperature. This comparison indicates that the breathing of the helix is a separate transition from the decrease in curvature of the dA tracts.

The shape function results also indicate that the curvatures of the dA tract containing DNAs do not appear to reach plateau values as the temperature is decreased. The evidence indicates that there is a continuum of observed curvature of dA tract DNA. The difference in shape functions between

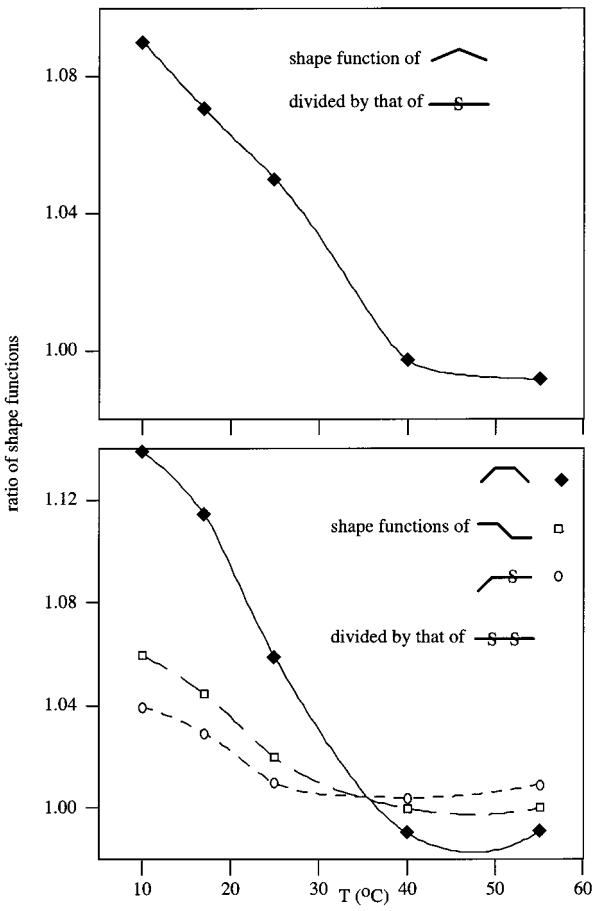

FIGURE 4: Ratio of the shape function of the DNA with a single, central dA tract to that of the DNA with a single, central scrambled sequence is shown as a function of temperature at the top. The ratios of the shape functions of the DNA with in or out of phase dA tracts to that of the DNA with two scrambled sequences is shown at the bottom. Also shown, is the ratio of the shape of the DNA with a dA tract and a scrambled sequence to that of the DNA with two scrambled sequences. The curves approximate the melting of the curvature of the dA tract DNAs. The points in both plots are connected by lines to aid visualization of the data and are not based on any model.

the DNAs with dA tracts and those with scrambled sequences continues to increase as the temperature is decreased down to the lowest temperatures examined. This indicates that the curvature is not only temperature dependent but that the curvature continues to increase as the temperature is decreased, perhaps until the sample freezes. Also, since the effect of curvature on the shape functions decreases by almost 50% when the temperature of the sample is raised from 10 to 25 °C, the energy associated with curvature must be quite small, on the order of a few kilocalories or less. In addition, the curvature melts out over a wide temperature range, indicating that there is not a cooperative transition between curved and noncurved DNA.

These shape function results do not distinguish between the various models for the origin of the curvature of the dA tract DNAs. The shape function results do not directly address whether the curvature is due to wedge or kink or other type of bending. The shape function results report on the average curvature and flexibility of the DNAs and not whether the DNA is undergoing rapid, on the time scale of NMR experiments, averaging between different conformational states.

A model has been developed to account for these and prior experimental results on dA tract DNAs. At low temperatures, below about 30 °C, the dA tract containing DNAs are curved and the extent of curvature increases with decreasing temperature. At a temperature of 40 °C, there is little curvature of the dA tract DNAs. By 55 °C, there is little difference between the hydrodynamics of DNAs with dA tracts and those with scrambled dA-dT regions.

There have been numerous studies on the effects of the curvature of dA tract DNAs. Almost all of these have considered the curvature of the DNAs to be a constant value. Many of the techniques used to monitor the curvature of DNA are limited to narrow ranges of temperature, buffer, and other environmental conditions. The curvature of DNA observed by X-ray diffraction is fixed at the time of crystallization. Gel retardation experiments are typically limited to a narrow temperature range as the properties of the gels are temperature dependent. Similarly, the rate of DNA cyclization may depend on the temperature dependence of the ligase as well as the properties of the DNA. The results presented here show that dA tracts do not have an intrinsic, temperature-independent curvature. Since dA tracts can adopt a continuous range of average curvature depending on the temperature, the curvature may be considered as a tendency to curve that depends on the temperature as well as the sequence.

There has been a prior proposal for the temperature dependence of the curvature of dA tracts (*52*, *53*). The circular dichroism, heat capacity, and decay of the slowest electric birefringence component of a 45mer duplex containing five dA_5 tracts were compared to the results on a 45mer duplex containing a randomized sequence. The dA-dT base pairs were randomly distributed throughout the duplex rather than having scrambled dA-dT regions as used here. On the basis of the experimental results, it was proposed that the curvature of dA tracts is temperature dependent and that the transition from curved to straight dA tract has a midpoint of about 30 °C. The enthalpy of curvature was estimated to be about 3.4 kcal/mol for each dA-dT base pair. Their description is largely in agreement with the model proposed here.

There are two differences between the prior interpretation and what is proposed here. One is that our model does not describe the curvature of dA tracts as two states but rather as a continuum of curved structures. The second is that the description of the temperature dependence of the curvature, and other properties of the dA tract DNAs, as determined by electric birefringence is somewhat different than that determined here. The rotation time of the random sequence sample exhibited an approximately 30% increase from 10 to 50 °C (*53*). Such a large change is difficult to understand. The origin of this temperature dependence was not clear (*53*), and this feature may have complicated the analysis. This temperature dependence may partially be due to the very low salt concentration, 1 mM Tris and 4 mM NaCl, used in the birefringence experiments. Also, the electric birefringence data was only collected on two DNAs. Nonetheless, the two models are overall in pretty good agreement.

There are additional data that qualitatively supports the temperature dependence of the curvature of dA tracts (*54*−*59*). For example, two recent reports have shown that the anomalous gel migration of synthetic (*58*) and natural

occurring DNAs (*57*) attributed to curvature appears to decrease with increasing temperatures.

Summary and Prospects. These results show that the curvature of dA tracts in duplex DNA is highly temperature dependent. In light of these results the description of the curvature of a dA tract as a specific value seems inappropriate. In contrast to these results, the flexibility induced by the presence of mismatched sites is mostly independent of temperature over the range that the curvature of dA tracts melts out. Taken together these results suggest that flexibility may be more important than curvature at physiological temperatures. It remains to be determined if the curvature of other sequences, such as dG tracts, is also highly temperature dependent and if magnesium, or the other cations found in cells, significantly stabilize the curvature of DNA.

The results also show that the examination of the shape functions of DNAs with damaged sites in or out of phase with respect to dA tracts will allow determination of the curvature of the damaged sites relative to that of a dA tract. The quantitative analysis of the results to determine the magnitude of the curvature as a function of temperature will require detailed modeling of the hydrodynamics of the DNAs and such an analysis will be undertaken.

The shape function approach can also be applied to the examination of whether minor groove binders alter the curvature of dA tract DNA as well as to the controversial issue of whether cations control the curvature of dA tract DNA. It may be the case that both the extent of curvature and the temperature dependence of the curvature of dA tract DNA are sensitive to the nature of the counterions. Our preliminary results indicate that magnesium increases the curvature of dA tracts as well as their thermal stability.

ACKNOWLEDGMENT

We would like to thank Don Albert for his help in providing the parts for the construction of the cooling unit that was used for the NMR experiments.

SUPPORTING INFORMATION AVAILABLE

Twenty-one additional figures. The first six contain the plots of $\ln(I_G/I_o)$ as a function of G^2, one for each of the DNAs, There is one figure comparing the use of peak intensity and integration on the plot of $\ln(I_G/I_o)$ as a function of G^2. Figure 8 is a plot of the shape function of water as a function of temperature. Figure 9 is the pulse sequence including the diffusion filter. Figure 10 shows the calibration of the gradient strength as a function of the duration of the gradient on time. Figures 11 and 12 show results obtained with and without the diffusion filter. Figure 13 contains plots of the spectra obtained for different gradient strengths to show that the spectral intensities in all regions are equally affected. Figures 14−19 contain the imino spectra of the six DNAs obtained at 10−55 °C. Figure 20 contains the plots of $\ln(I_G/I_o)$ as a function of G^2 for all six DNAs at 10 °C and Figure 21 contains a depiction of the modeling for the melting of the curvature of dA tracts.

REFERENCES

1. Marathias, V. M., Jerkovic, B., and Bolton, P. H. (1999) *Nucleic Acids Res. 27*, 1854−1858.
2. Marathias, V. M., Jerkovic, B., Arthanari, H., and Bolton, P. H. (2000) *Biochemistry 39*, 153−160.
3. Harrington, R. E. (1993) *Electrophoresis 14*, 732−746.
4. Cleaver, J. E., and States, J. C. (1997) *Biochem. J. 328*, 1−12.
5. Huertas, M. L., Navarro, S., Lopez Martinez, M. C., and Garcia de la Torre, J. (1997) *Biophys. J. 73*, 3142−3153.
6. Crothers, D. M. (1998) *Proc. Natl. Acad. Sci. U.S.A. 95*, 15163−15165.
7. de Souza, O. N., and Ornstein, R. L. (1998) *Biopolymers 46*, 403−415.
8. Georghiou, S., Kubala, S. M., and Large, C. C. (1998) *Photochem. Photobiol. 67*, 526−531.
9. Grove, A., Galeone, A., Mayol, L., and Geiduschek, E. P. (1996) *J. Mol. Biol. 260*, 196−206.
10. Harvey, S. C., Dlakic, M., Griffith, J., Harrington, R., Park, K., Sprous, D., and Zacharias, W. (1995) *J. Biomol. Struct. Dyn. 13*, 301−307.
11. Kahn, J. D., and Crothers, D. M. (1993) *Cold Spring Harbor Symp. Quant. Biol. 58*, 115−122.
12. Kahn, J. D., Yun, E., and Crothers, D. M. (1994) *Nature 368*, 163−166.
13. Goodman, S. D., and Kay, O. (1999) *J. Biol. Chem. 274*, 37004−37011.
14. Okonogi, T. M., Reese, A. W., Alley, S. C., Hopkins, P. B., and Robinson, B. H. (1999) *Biophys. J. 77*, 3256−3276.
15. Richmond, T. J., and Steitz, T. A. (1998) *Curr. Opin. Struct. Biol. 8*, 11−13.
16. Luger, K., and Richmond, T. J. (1998) *Curr. Opin. Struct. Biol. 8*, 33−40.
17. Maher, L. J., III (1998) *Curr. Opin. Chem. Biol. 2*, 688−694.
18. Anselmi, C., Bocchinfuso, G., De Santis, P., Savino, M., and Scipioni, A. (1999) *J. Mol. Biol. 286*, 1293−1301.
19. Bechert, T., Heck, S., Fleig, U., Diekmann, S., and Hegemann, J. H. (1999) *Nucleic Acids Res 27*, 1444−1449.
20. Cognet, J. A., Pakleza, C., Cherny, D., Delain, E., and Cam, E. L. (1999) *J. Mol. Biol. 285*, 997−1009.
21. Hagerman, P. J. (1990) *Annu. Rev. Biochem. 59*, 755−781.
22. Schatz, T., and Langowski, J. (1997) *J. Biomol. Struct. Dyn. 15*, 265−275.
23. Sitlani, A., and Crothers, D. M. (1998) *Proc. Natl. Acad. Sci. U.S.A. 95*, 1404−1409.
24. Tung, C. S., and Harvey, S. C. (1986) *J. Biol. Chem. 261*, 3700−3709.
25. Calladine, C. R., and Drew, H. R. (1996) *J. Mol. Biol. 257*, 479−485.
26. Carrera, P., Martinez-Balbas, M. A., Portugal, J., and Azorin, F. (1991) *Nucleic Acids Res. 19*, 5639−5644.
27. De Santis, P., Fua, M., Palleschi, A., and Savino, M. (1995) *Biophys. Chem. 55*, 261−271.
28. Diekmann, S. (1992) *Methods Enzymol. 212*, 30−46.
29. Dlakic, M., and Harrington, R. E. (1995) *J. Biol. Chem. 270*, 29945−29952.
30. Dlakic, M., and Harrington, R. E. (1998) *Nucleic Acids Res. 26*, 4274−4279.
31. Goodsell, D. S., and Dickerson, R. E. (1994) *Nucleic Acids Res. 22*, 5497−5503.
32. Hagerman, P. J. (1984) *Proc. Natl. Acad. Sci. U.S.A. 81*, 4632−4636.
33. Martinez-Balbas, A., Rodriguez-Campos, A., Garcia-Ramirez, M., Sainz, J., Carrera, P., Aymami, J., and Azorin, F. (1990) *Biochemistry 29*, 2342−2348.
34. Stellwagen, N. C. (1997) *Electrophoresis 18*, 34−44.
35. Strauss, J. K., and Maher, L. J., III (1994) *Science 266*, 1829−1834.
36. Trifonov, E. N. (1985) *CRC Crit. Rev. Biochem. 19*, 89−106.
37. Ross, E. D., Den, R. B., Hardwidge, P. R., and Maher, L. J., III (1999) *Nucleic Acids Res 27*, 4135−4142.
38. Barkley, M. D., and Zimm, B. H. (1979) *J. Chem. Phys. 70*, 2991−3007.
39. Chiu, T. K., Kaczor-Grzeskowiak, M., and Dickerson, R. E. (1999) *J. Mol. Biol. 292*, 589−608.
40. McFail-Isom, L., Sines, C. C., and Williams, L. D. (1999) *Curr. Opin. Struct. Biol. 9*, 298−304.

41. Lapham, J., Rife, J. P., Moore, P. B., and Crothers, D. M. (1997) *J. Biomol. NMR 10*, 255−262.
42. Waring, M. J., and Bailly, C. (1994) *J. Mol. Recognit. 7*, 109−122.
43. Walker, W. L., Kopka, M. L., and Goodsell, D. S. (1997) *Biopolymers 44*, 323−334.
44. Lown, J. W. (1994) *J. Mol. Recognit. 7*, 79−88.
45. Ha Duong, T., and Zakrzewska, K. (1997) *J. Biomol. Struct. Dyn. 14*, 691−701.
46. Bailly, C., and Chaires, J. B. (1998) *Bioconjugate Chem. 9*, 513−538.
47. Young, M. A., Goljer, I., Kumar., S., Srinivasan, J., Beveridge, D. L., and Bolton, P. H. (1995) *Methods Enzymol. 261*, 121−144.
48. DiGabriele, A. D., Sanderson, M. R., and Steitz, T. A. (1989) *Proc. Natl. Acad. Sci. U.S.A. 86*, 1816−1820.
49. DiGabriele, A., and Steitz, T. A. (1993) *J. Mol. Biol. 231*, 1024−1039.
50. Kahn, J. D., and Crothers, D. M. (1998) *J. Mol. Biol. 276*, 287−309.
51. Crothers, D. M., Drak, J., Kahn, J. D., and Levene, S. D. (1992) *Methods Enzymol. 212*, 3−29.
52. Chan, S. S., Breslauer, K. J., Hogan, M. E., Kessler, D. J., Austin, R. H., Ojemann, J., Passner, J. M., and Wiles, N. C. (1990) *Biochemistry 29*, 6161−6171.
53. Chan, S. S., Breslauer, K. J., Austin, R. H., and Hogan, M. E. (1993) *Biochemistry 32*, 11776−11784.
54. Herrera, J. E., and Chaires, J. B. (1989) *Biochemistry 28*, 1993−2000.
55. Katayama, S., Matsushita, O., Jung, C. M., Minami, J., and Okabe, A. (1999) *EMBO J. 18*, 3442−3450.
56. Rivetti, C., Walker, C., and Bustamante, C. (1998) *J. Mol. Biol. 280*, 41−59.
57. Rohde, J. R., Luan, X. S., Rohde, H., Fox, J. M., and Minnich, S. A. (1999) *J. Bacteriol. 181*, 4198−4204.
58. Ussery, D. W., Higgins, C. R., and Bolshoy, A. (1999) *J. Biomol. Struct. Dyn. 16*, 811−823.
59. Volker, J., Blake, R. D., Delcourt, S. G., and Breslauer, K. J. (1999) *Biopolymers 50*, 303−318.

BI0014507